JOURNAL OF SOLID STATE CHEMISTRY 98, 223–236 (1992)

A Geometric Model of Deviations from Vegard's Rule

VADIM S. URUSOV

Department of Crystallography and Crystal Chemistry, Geological Faculty, Moscow State University, 119899 Moscow, Russia

Received June 10, 1991; in revised form September 23, 1991

There is much evidence that X-ray measurements of sufficient accuracy reveal deviations from the linear dependence of unit-cell parameters on composition, i.e., departures from Vegard's rule. The dependence of such deviations on composition for a random solid solution with one substitutional position $(A_{x_1}B_{x_2})C$ is usually of a parabolic form: $\delta a = x_1 x_2 \sigma$, where σ is positive. Many attempts to explain these observations are based on elastic models. It is known that less than 50% of the predictions of these models are correct. An alternative model under consideration is a simple geometric one. It is concerned with secondary atomic displacements around substitutional defects, i.e., shifts of the second nearest neighbors. The result is structurally dependent and the analysis deals with binary solid solutions of $B1$ (CN = 6), $B3$ (CN = 4), and $B2$ (CN = 8) structure types. For instance, in sodium chloride structure-type solid solutions, the following simple equation is valid,

$$\delta h = (3/2)x_1 x_2 (\Delta R)^2/R,$$

where ΔR is the difference in interatomic distances of pure components and R is the average interatomic distance. Calculations for NaCl–KCl, NaCl–NaBr, KCl–KBr, and other systems are in good agreement with experimental data.

Introduction

The 70 years following Vegard's discovery (*1*) of a linear dependence of the unit cell parameters in a solid solution, $(A_{x_1}B_{x_2})C$, on the composition of that solution,

$$a = x_1 a_1 + x_2 a_2 \qquad (1)$$

(a, a_1, and a_2 are unit cell parameters of a solid solution and end-members, x_1 and x_2 are molar fractions of end-members, AC and BC), have witnessed not only a lot of support for this rule but also a number of deviations from it as well. Generally, with increasing experimental accuracy the cases of deviation from Vegard's rule grow in number.

Numerous attempts were made (*2–5*) to explain and predict deviations from Vegard's rule. Most of them based on the theory of elasticity of elongation and shear (*2–4*) are concerned with binary metal alloys. The analysis of these models (*6*) shows that the proportion of correct predictions is small, about 40% on the average. In Ref. (*7*) a model based on the theory of elasticity was, however, successfully applied to the explanation of the deviations from Vegard's rule observed for the system TiO_2 (rutile)–SnO_2 (cassiterite). Somewhat earlier (*8*) the reasons for deviations from Vegard's rule for essentially ionic solid solutions (halogenides, oxides, etc.) were subdivided into geometrical and chemical.

0022-4596/92 $5.00

If atomic substitution occurs in several symmetry nonequivalent structural sites, deviations from Vegard's rule (including negative and sign-variable deviations) can often be explained by the preferential occupation of one or several sites (*9*). The validity conditions of Vegard's rule for multipositional solid solutions such as perovskite (*10, 11*) or spinel (*12–14*) were determined by means of the model of quasielastic bonds.

Slight positive deviations can be described by the volume additivity rule (Retger's rule) (*15*):

$$a^3 = x_1 a_1^3 + x_2 a_2^3. \qquad (2)$$

In most cases the observed deviations exhibit a parabolic composition dependence

$$a = x_1 a_1 + x_2 a_2 + \Delta a$$
$$= x_1 a_1 + x_2 a_2 + x_1 x_2 \sigma. \qquad (3)$$

The purpose of the present report is to analyze possible geometric reasons for deviations from Vegard's rule in the case of unipositional substitutional solid solutions (insulators and semiconductors).

Local Displacements of Atoms in the Solid Solution Structure

If a solid solution obeys Vegard's rule (*1*), the average bond lengths in its structure can be found from the analogous additivity rule

$$R(x) = \overline{R}_1(x) = \overline{R}_2(x) = x_1 R_1 + x_2 R_2$$
$$= R_2 - x_1 \Delta R = R_1 + x_2 \Delta R, \qquad (4)$$

where R_1 and R_2 are the interatomic distances in the end-members AC and BC, and $\Delta R = R_2 - R_1$. The assumption that all of the individual bond lengths in the mixed crystal are equal to their average values according to rule (*4*), i.e., relaxation is completely absent, $\varepsilon = 0$, corresponds to the idea of the so-called virtual crystal (Fig. 1).[1]

[1] $\varepsilon = (R_{BC} - R^0_{AC})/(R^0_{BC} - R^0_{AC})$, where R_{BC} is the BC bond length around the B impurity in the AC host crystal, and R^0_{AC} and R^0_{BC} are bond lengths of pure end-members AC and BC, respectively.

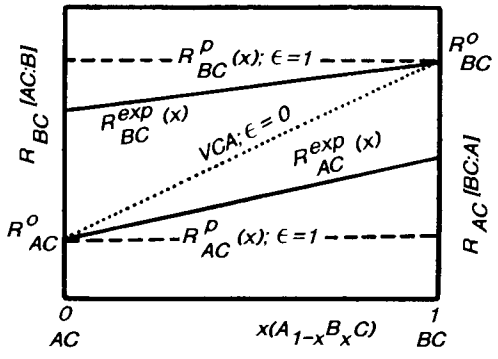

FIG. 1. A schema of A–C and B–C bond length changes dependent on composition. VCA, virtual crystal approximation, no relaxation, $\varepsilon = 0$, Vegard's rule is fulfilled; R^p, full relaxation, $\varepsilon = 1$, individual bond lengths are equal to those for end members; and R^{exp}, real changes in individual bond lengths as a function of composition.

Under another assumption all the atoms in the solid solution conserve their initial sizes, i.e., with the structure relaxation being at a maximum ($\varepsilon = 1$) the individual bond lengths are equal to the bond lengths in the end-members R_1 and R_2. This assumption underlies the model of bond alternation.

Both above extreme cases agree equally well with Vegard's rule, which is schematically shown in Fig. 1. It is clear that the actual changes in the bond lengths of various sorts must lie between the limits mentioned. In other words, partial relaxation of the structure does not contradict Vegard's rule (Fig. 1).

The determination of the degree of structure relaxation, i.e., the local displacements of atoms, is an independent, complicated enough, experimental and theoretical problem. It is especially difficult to obtain information on local structure by traditional methods which carry information on average atomic coordinates. Nevertheless, the early X-ray diffraction study of solid solutions KCl–KBr and KCl–RbCl (1 : 1) undertaken by J. A. Wasastjerna (*16*) detected a decrease in reflection intensities compared

to the case of end-member crystals. This fact cannot be explained only by thermal vibrations and requires the assumption of noticeable static displacements of ions from their ideal positions. Particularly large local displacements, of the order of the difference between the interatomic distances of end members, proved to be experienced by the atoms in the mixed arrangement (K in the first and Cl in the second case). An X-ray study of alloys (*17*) demonstrated that if the mixed crystal retains the space symmetry of end members, a decrease in intensities of reflections and the emergence of diffuse scattering regions near them speak in favor of the local deformation of the alloy structure within several bond lengths around the impurity atom. An analysis of such effects (*18*) showed that local displacements are of the order of the difference of interatomic distances; no strict correlation, however, was observed between them.

It was about 10 years ago when it became possible to directly determine individual bond lengths in mixed crystals by the EXAFS (extended X-ray absorption fine structure) method. In 1979–1980 this method allowed considerable local displacements of atoms around impurities to be detected in metal alloys and then in mixed halogenides. As an example, Fig. 2a illustrates the experimental composition dependencies of the nearest distances Ga–As and In–As in the sphalerite-structure solid solution (Ga, In)As (its coordination number being equal to 4) (*19*). As can be seen, the maximum change in bond length corresponding to the dilute solution amounts only to 20–25% of the difference $\Delta R = R_2 - R_1$ ($R_2 > R_1$) between the bond lengths in the end members. Thus, the actual interatomic distances considerably differ from distances in the virtual crystal model, though the weighted mean of these distances is nearly exactly described by Vegard's rule.

It was also observed in that experiment (*19*) that the distributions of the Ga–As and

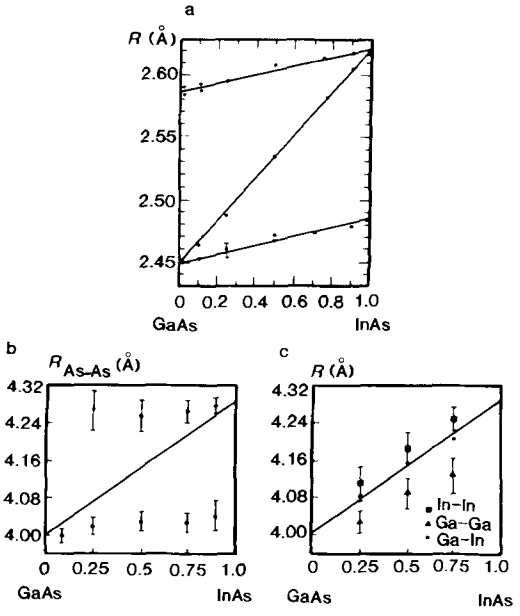

FIG. 2. Changes in interatomic distances in ($Ga_x In_{1-x}$) As solid solution by EXAFS data (*19*). *a*, distances between nearest neighbors In–As and Ga–As. Average distances $R = x_1 R_{In-As} + x_2 R_{Ga-As}$ are in agreement with Vegard's rule; *b*, distances between second nearest neighbors As–As; *c*, distances between second nearest neighbors In–In, Ga–Ga, and Ga–In.

In–As distances in the solid solution are nearly the same as in the end members, which is in accordance with the fact that the nearest environment of both cations is uniform and consists only of arsenic atoms. As distinct from this, there occurs a bimodal distance distribution around the As atoms which correspond to the mixed cation (Ga, In) environment of this atom.

The distances between the second nearest neighbors (cation–cation, anion–anion) considerably differ in their character. EXAFS data indicate the existence of two different As–As distances in the solid solutions: short distances correspond to the As–Ga–As configuration and longer distances to the As–In–As configuration (Fig. 2b). The weighted mean of these two distances corresponds to Vegard's rule (the

solid line in Fig. 2b). It is clear that the anion packing in the solid solution is strongly distorted compared to the regular cubic (close) packing of anions in the end members.

A different picture is observed in the case of the distances of the cation–cation second nearest neighbors. As can be seen from Fig. 2c all the interatomic distances Ga–Ga, In–In, and In–Ga vary to obey Vegard's rule (within deviations of the order of 0.05 Å), which follows from the virtual crystal model. This means that the atoms in the mixed (cation) sublattice, as opposed to those in the nonmixed (anion) sublattice, occupy nearly regular positions, and distortions of the ideal packing are relatively slight.

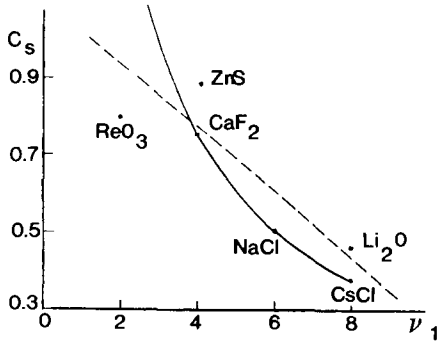

FIG. 3. Correlation between site compliance parameter C_s and first coordination number ν_1. Solid line, calculated, Eq. (15); points, DLS model; dashed line, averaged, DLS.

Very similar results were also obtained with EXAFS for ionic solid solutions of the NaCl (CN = 6) structural type: (K, Rb)Br and Rb(Br, I) (*20*). However, in both cases the maximum change in distances is about twice that for essentially covalent crystals of the ZnS structural type; viz., it amounts to about 40%. Relatively large changes in distances, about 40%, were also observed for Sr-substituted fluorite CaF_2 (*21*). In these solutions the mixed sublattice can also be viewed as a slightly distorted packing and the common atoms being displaced from the ideal positions. The local structure of a solid substitutional solution observed by EXAFS is in good agreement with numerous theoretical calculations of structural distortions around the impurity in an ionic crystal (*22–26*). A typical result of such calculations is the fact that the displacement of the nearest neighbors around the impurity in the NaCl structure is equal to nearly half the difference between the interatomic distances: $\delta R \simeq \frac{1}{2}\Delta R$. The displacement of the second and more distant neighbors decreases approximately proportionally to the square of interatomic distances, which is the consequence of the model of elastic continuum (*27*).

A more detailed picture of local displacements is obtainable by DLS modeling which consists in the least-squares optimization of individual bond lengths, i.e., their fitting some standard distances (which represent distances in end members in the case of solid solutions). The application of DLS modeling to isovalent solid solutions of different structures made it possible for Dollase (*28*) to introduce the notion of "site compliance." This means the actual proportion of increase (or decrease) in the bond length relative to the difference of the bond lengths in the end members in the limit of infinite dilution (a very small amount of impurity atoms). Dollase made the conclusion (*28*) that the compliance parameter c_s is inversely proportional to the coordination number of the nearest neighbors of the impurity because they suffer the largest displacement (Fig. 3). Thus, less close-packed structures (ZnS, ReO_3) are characterized by large changes in bond lengths, whereas close-packed ones (NaCl, CsCl) exhibit small changes in bond lengths. It should be noted that the calculations by the DLS method agree well with experiments. Thus, for example, the predicted relaxation of bond lengths in the NaCl structural type is about 50% and in the ZnS-type solid solutions is close to 20%, these results being

close to experimental findings (40–50% and 20–25%, respectively).

Primary Displacements in Simple Structures

As follows from the experimental and theoretical results considered above, the largest displacements in a solid solution structure $(A_{x_1}B_{x_2})C$ are experienced by atoms C in that sublattice where no mixing takes place. As regards atoms A and B, they form the nearly nondistorted packing. Other consequences of this assumption are as follows.

If the environment of the common atom C is uniform, i.e., if it consists either of atoms A or of atoms B, then all the distances A–C or B–C are the same and equal to the mean $R(x)$ (see formula (4)). If the environment of the atom C is mixed, i.e., consists of some atoms A and B, then bond chains A–C–B appear in the structure and the atom C is displaced from its ideal position midway between its neighbors toward the smaller atom. Let, for example, the atom A to be larger than B. In this case, the atom C is displaced from the center of the A–C–B chain toward B and the distance A–C becomes equal to $R + u$, where u is a certain displacement of the atom C.

A change in the distance C–B in the A–C–B chain is dependent on the bond angle $<A$–C–B and can be represented in a first order approximation as

$$u_1 = u \cos \alpha, \tag{5}$$

where $\alpha = <A$–C–B. Let us call these displacements primary ones.

In the NaCl structure (an octahedral arrangement) the A–C–B chain is linear, $\alpha = 180°$C, and, consequently, $u_1 = -u$. In the ZnS structure (a tetrahedral coordination) $\alpha = 109°28'$ and, therefore, $u_1 = -(1/3)\,u$.

In the CsCl structure with a cubic environment of the central atom there exist three types of chains with the angles 180°, 109°28′, and 70°32′. From Eq. (5) it follows that in this case

$$u_1 = -u,$$

$$u_1' = \pm\tfrac{1}{3}\,u.$$

Thus, in a first order approximation, the bond lengths around the impurity in the NaCl structural type become mutually compensated, due to their changes, by $+u$ and $-u$, respectively. In the ZnS structural type the displacement of the common atom along one of the bond lines by an amount of u is compensated for by changes in each of the other three bond lengths by $-\frac{1}{3}\,u$. In the CsCl structural type the displacement of an atom from the cube center makes the length of one bond increase by u and that of the other bond decrease simultaneously by $-u$. In addition, an increase in the bond length by u is accompanied by a reduction of the other three bonds by $-\frac{1}{3}\,u$, and a decrease in the bond length by $-u$ is accompanied by an elongation of the other three bonds by $\frac{1}{3}\,u$. In other words, primary displacements completely compensate for one another and cannot be the reason for deviations from Vegard's rule.

Radial Force Model of a Random Solid Solution

Now let us try to estimate primary displacements using the simple model of radial forces. Denote by $e\,(R)$ the energy of a certain pair of bound atoms separated by a distance R from each other. The number of the A–C bonds in the A–C–A chains is proportional to the probability of their occurrence in the solid solution, i.e., to x_1^2, their number in the A–C–B chains being proportional to x_1x_2. Similarly, the number of the B–C bonds in the B–C–B chains is proportional to x_2^2 and their number in the B–C–A chains to x_2x_1.

The energy change in the formation of the solid solution may be represented as

$$\Delta E = N\nu\{x_1^2[e_1(R) - e_1(R_1)] + x_2^2[e_2(R) - e_2(R_2)] + x_1x_2\{e_1(\overline{R}_1) - e_1(R_1)] + x_2x_1[e_2(\overline{R}_2) - e_2(R_2)]\}. \quad (6)$$

Here N is Avogadro's number, ν is the coordination number, $e_1(R_1)$ and $e_2(R_2)$ are the bond energies in the end members, $e_1(R)$ and $e_2(R)$ are the energies of two bond types (A–C and B–C) at a mean distance R in symmetric bond chains, and $e_1(\overline{R}_1)$ and $e_2(\overline{R}_2)$ are the energies of these bond types in nonsymmetric bond chains.

The distances $\overline{R}_1$ and $\overline{R}_2$ depend on displacements of C atoms in accordance with the bond angles as shown in the previous section. For example, for the NaCl structure

$$\overline{R}_2 = R + u,$$
$$\overline{R}_1 = R - u.$$

Expand the energy ΔE into a Taylor series. Leaving the first and second order terms and taking into account that the first derivative $e'(R) = 0$ (at $T = 0$ K) in the equilibrium state, we have

$$e(R) - e(R_0) = \tfrac{1}{2}e''(R_0)(R - R_0)^2.$$

If we assume that the properties of the components are close, i.e., $e_1''(R_1) \simeq e_2''(R_2) = e''(R)$, we obtain from (6) that

$$\Delta E = \tfrac{1}{2}N\nu e''(R)[x_1^2(R - R_1)^2 + x_2^2(R - R_2)^2 + x_1x_2(R - R_1 - u)^2 + x_1x_2(R - R_2 + u)^2]. \quad (7)$$

Using Vegard's rule in form (4) we can rewrite expression (7) as follows

$$\Delta E = \frac{x_1x_2}{2}N\nu e''(R)[2x_1x_2(\Delta R)^2 + (x_2\Delta R - u)^2 + (x_1\Delta R + u)^2]. \quad (8)$$

Minimizing ΔE as a function of the displacement u we arrive at the condition

$$\frac{d\Delta E}{du} = \frac{x_1x_2}{2}N\nu e''(R)[-2x_2\Delta R + 2u - 2x_1\Delta R + 2u] = 0,$$

wherefrom $4u = 2\,\Delta R(x_1 + x_2)$. As $x_1 + x_2 = 1$, finally we have

$$u = \tfrac{1}{2}\Delta R. \quad (9)$$

This result means that the displacement of the common atom in the NaCl structure amounts to half the difference of the interatomic distances in the end members. This estimate is close to the experimental data reported in (*20*) and to the compliance parameter of the DLS method (*28*).

In solid solutions of the ZnS structural type the displacement of the common atom in the case of its nonsymmetrical environment, i.e., in the A–C–(B) chain, by an amount of u is connected with the simultaneous change in the length of the other three bonds B–C by $-\frac{1}{3}u$. Thus, the individual bond lengths

$$\overline{R}_2 = R + u = R_2 - x_1\Delta R + u,$$
$$(3\times)\overline{R}_1 = R - \tfrac{1}{3}u = R_1 + x_2\Delta R - \tfrac{1}{3}u. \quad (10)$$

Earlier the model of radial force field was used (*29*) for the mixed tetrahedral coordination of a central atom and the following value of the primary displacement was obtained:

$$u = \tfrac{3}{4}\Delta R. \quad (11)$$

The primary displacement obtained is in agreement with the atomic displacements observed by EXAFS (20–25% of the bond length difference in the end members) and with the predictions of the DLS method (*28*) (the compliance parameter $c_s = 0.84$).

As shown in the preceding section, in solid solutions of the CsCl structural type each primary displacement $\pm u$ is accompanied by three displacements $\mp\frac{1}{3}u$. Therefore, the total energy change in the approximation of radial forces may be expressed as

$$\Delta E = \frac{x_1x_2}{2}N\nu e''(R)\left[2x_1x_2(\Delta R)^2 + (x_1\Delta R - u)^2 + (-x_2\Delta R + u)^2 + 6\left(\frac{u}{3}\right)^2\right]. \quad (12)$$

Minimizing (12) as a function of u yields

$$\frac{d\Delta E}{du} = \frac{x_1 x_2}{2} N\nu e''(R)(-2x_1\Delta R + 2u - 2x_2\Delta R + 2u + \tfrac{4}{3}u) = 0, \quad (13)$$

wherefrom $u = \frac{3}{8}\Delta R$.

This result is also in good agreement with the estimate of the site compliance in the CsCl structure: $c_s = 0.38$ (*28*) (cf. $\frac{3}{8} = 0.375$).

Generalizing the above estimates of primary displacements of the central atom in the coordination polyhedron in the case of its nonsymmetric environment, we may write the expression

$$u = \frac{3}{\nu_1}\Delta R, \quad (14)$$

where ν_1 is the first coordination number. This is in agreement with Dollase's conclusion (*28*) that the site compliance is inversely proportional to the number of ligands. In other words, we have the following simple relation between c_s and ν_1,

$$c_s = 3/\nu_1, \quad (15)$$

which is compared (Fig. 3) with the DLS results. As seen, significant deviations from the solid line calculated by Eq. (15) reveal those structures (Li_2O, ReO_3) which are not analyzed in present paper.

Secondary Displacements and Deviations from Vegard's Rule

Primary displacements of the neighbors of the central atom in a mixed coordination polyhedron, which may be estimated by formula (*14*), entail displacements of the second and higher orders. Let us consider an octahedral arrangement with one substituted atom in the vertex of a regular octahedron if the assumption is made of the regular

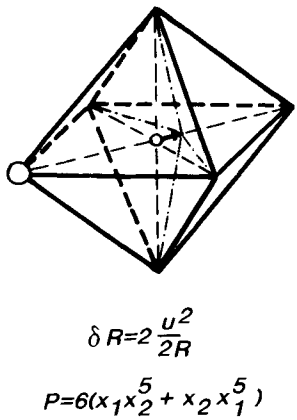

FIG. 4. Octahedral arrangement of an atom shifted from center with one substituted ligand. δR, change of distances between second nearest neighbors; P, probability of the configuration.

undistorted packing of the mixed sublattice (Fig. 4). As can be seen, the displacement of the atom C from the octahedron center along the bond causes changes not only in the two bond lengths by amounts $+u$ and $-u$, respectively, but also in the other four bond lengths. It can easily be found that the change in the symmetric bond length is $\delta_1 = \sqrt{R^2 + u^2} - R \simeq u^2/2R$ (to second order terms, i.e., secondary displacements). In the case of two substituted atoms in the octahedron (Fig. 5) all the bonds experience additional secondary displacements by $\delta_2 = u^2/R$ and in the case of three substituted atoms (Fig. 6) by $\delta_3 = 3\,u^2/2R$.

The general expression for secondary displacements is as follows: $\delta_i = (i/2)(u^2/R)$ ($i = 1, 2, 3$). The doubled and trebled displacements for $i = 2$ and $i = 3$, respectively, are connected with the fact that all of the ligands become the second nearest neighbors of two ($i = 2$) or three ($i = 3$) substituents.

The proportion of various configurations for different compositions can be calculated by the binomial formula

$$P = (x_1 + x_2)^{\nu}. \quad (16)$$

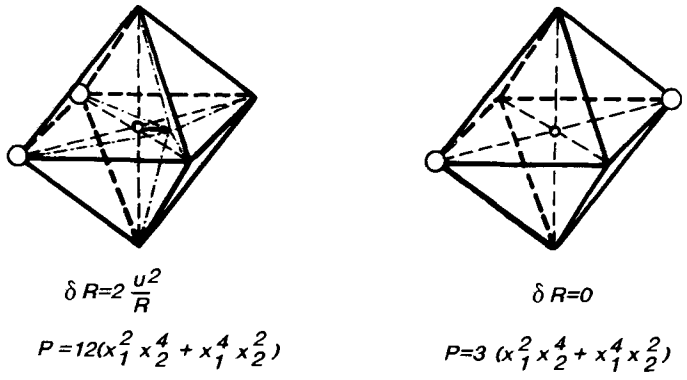

FIG. 5. Octahedral arrangement with two substituted ligands and corresponding displacements δR and probabilities P.

The probabilities of individual configurations are determined by the expression

$$P_i = m_i x_1^{\nu-\omega} x_2^{\omega}, \tag{17}$$

where ω is the amount of atoms of the other sort in the polyhedron vertices and m_i is the multiplicity of a given configuration (the corresponding coefficient in the binomial theorem). The multiplicities m_i can be found from the relation

$$m_i = \frac{n_i}{n}, \tag{18}$$

where n is the symmetry order of the regular coordination polyhedron and n_i is the symmetry order of the ith configuration ("substituted" polyhedron). Thus, for instance, the multiplicity of the first configuration in Fig. 4 is

$$m_1 = \frac{48}{8} = 6,$$

because 48 is the symmetry ($m3m$) order of the regular octahedron and 8 is the symmetry ($4\,mm$) order of the one-substituted octahedron.

It should be noted that secondary displacements refer to the distances between

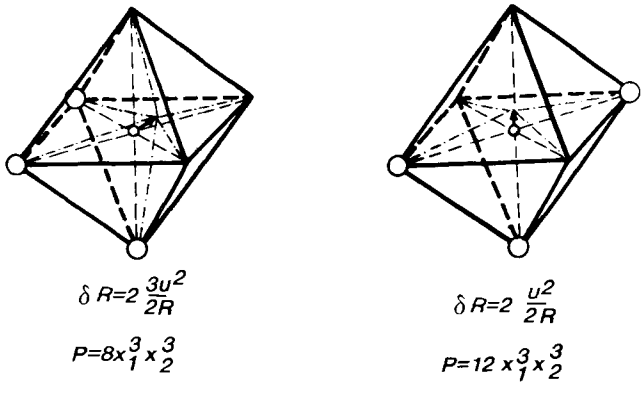

FIG. 6. Octahedral arrangements with three substituted ligands and corresponding displacements δR and probabilities P.

the central atom and second neighbors of the substitutional defect and that formulas (16) and (17) determine the probabilities of primary displacements. The number of secondary displacements is to the number of primary displacements as $l = \nu_2/\nu_1$, where ν_1 and ν_2 are the first and second coordination numbers, respectively. Therefore, the relative probabilities of secondary displacements can be calculated by the formula

$$P_i' = m_i l x_1^{\nu-\omega} x_2^{\omega}. \tag{19}$$

Now it is possible to obtain the final equation

$$\delta R = \sum_i P_i' \delta_i. \tag{20}$$

Taking into account that $l = 12/6 = 2$ for NaCl ($B1$) and using the above quantities $\delta_i = iu^2/2R$ ($i = 1, 2, 3$) we may reduce sum (20) to the form

$$\delta R_{B1} = 6 x_1 x_2 \left(\frac{u^2}{R}\right). \tag{21}$$

It was found in the preceding section that $u = \Delta R/2$ for the NaCl structural type. Accordingly,

$$\delta R_{B1} = \tfrac{3}{2} x_1 x_2 \frac{(\Delta R)^2}{R}. \tag{22}$$

In the case of a tetrahedral arrangement there occur two configurations: with one and with two substituents, Fig. 7. The corresponding primary and secondary displacements and their probabilities are presented in Fig. 7. The ratio of the numbers of secondary and primary displacements $l = 3$ in accordance with the ratio $\nu_2/\nu_1 = 12/4 = 3$.

Summation (20) yields in this case

$$\delta R_{B3} = 4 x_1 x_2 \left(\frac{u^2}{R}\right), \tag{23}$$

and, subject to $u = \frac{3}{4} \Delta R$ for the ZnS ($B3$) structure, we have

$$\delta R_{B3} = \tfrac{9}{4} x_1 x_2 \frac{(\Delta R)^2}{R}. \tag{24}$$

The cubic arrangement in the CsCl ($B2$) structure allows 13 configurations with substitutions in one, two, three, and four vertices of the cube. The corresponding primary and secondary displacements and their probabilities are presented in Figs. 8–11. For structure $B2$ the ratio of the number of secondary displacements to that of primary displacements is $l = 3.25$ in accordance with the fact that the second ($\nu_2 = 6$), third ($\nu_3 = 12$), and fourth ($\nu_4 = 8$) neighbors of substitutional defects take part in these displacements. In this case summation (20) yields

$$\delta R_{B2} = 8 x_1 x_2 \left(\frac{u^2}{R}\right). \tag{25}$$

With $u = \frac{3}{8} \Delta R$ for structure $B2$ in mind, we arrive at the expression

$$\delta R_{B2} = \tfrac{9}{8} x_1 x_2 \frac{(\Delta R)^2}{R}. \tag{26}$$

Equations (21), (23), and (25) can be written in general form

$$\delta R = \nu_1 x_1 x_2 \left(\frac{u^2}{R}\right), \tag{27}$$

whereas Eqs. (22), (24), and (26) in the form

$$\delta R = \frac{9}{\nu_1} x_1 x_2 \frac{(\Delta R)^2}{R}. \tag{28}$$

Comparison of the Geometric Model with Experimental Evidence

Few measurements of the composition dependence of the lattice parameter are reported for solid solutions of the CsCl structural type. The deviations from Vegard's rule observed in CsCl–CsBr did not exceed ± 0.002 Å for all compositions (*30–32*). The estimate by formula (26) yields the following result: the maximum deviation for the com-

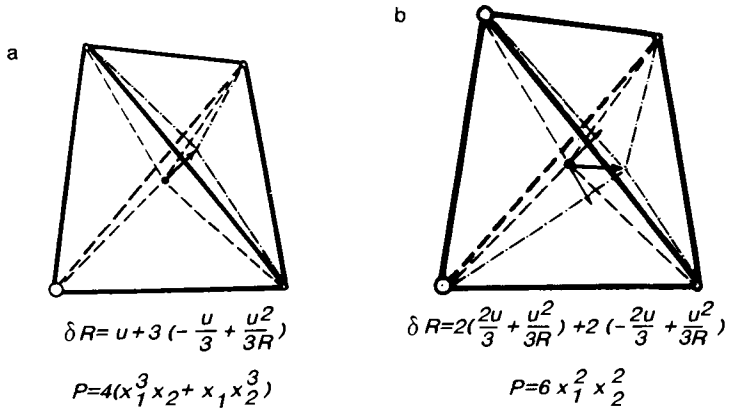

FIG. 7. Tetrahedral arrangements with one (a) and two (b) substituted ligands and corresponding δR and P.

position of $x_1 = x_2 = 0.5$ amounts to $+0.0017$ Å, which does not contradict the experimental evidence.

Reference (*33*) reports the experimental results of the composition dependence of the unit cell parameters for low-temperature (structure $B2$) and high-temperature (structure $B1$) solid solutions NH_4Cl–NH_4Br. Positive deviations from Vegard's rule for intermediate compositions ($x = 0.5$) of the low-temperature series reach about 0.004 ± 0.002 Å (high-angle measurements). Formula (26) gives 0.002 Å, this being in agreement with experiment.

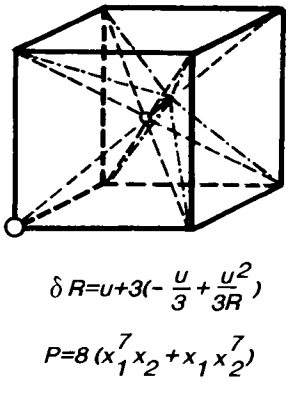

FIG. 8. Cubic arrangement with one substituted ligand and displacements δR and probability P.

A considerably larger number of measurements have been made for solid solutions of the NaCl structural type. Table I compares the deviations from Vegard's rule measured for four systems with those estimated by Eq. (22). As can be seen, the agreement between theory and experiment is very good.

Less accurate measurements were made for systems KCl–RbCl (*38*) and KBr–KI (*39*). Positive deviations of interatomic distances from the additivity rule in the first system lie within the interval 0.001–0.008 Å, whereas their theoretical values are contained within a narrower interval of 0.001–0.003 Å. For the second system, the spread of experimental deviations forms a wider interval from -0.001 to 0.017 Å. The deviations calculated by Eq. (22) do not exceed 0.006 Å.

Extensive investigations were made of the composition dependence of the unit cell parameters for solid solutions of the sphalerite ($B3$) and wurtzite ($B4$) structures. The results of these measurements made with different degrees of accuracy are sometimes contradictory. Thus, for instance, both posi-

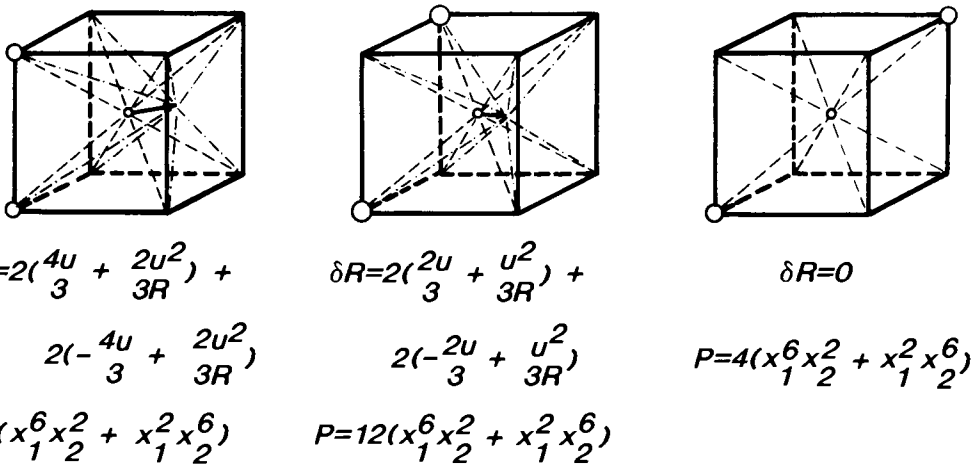

FIG. 9. Cubic arrangements with two substituted ligands and corresponding displacements δR and probabilities P.

tive and negative deviations from Vegard's rule were observed for the ZnS–CdS ($B4$) system; however, most of the measurements agreed with Vegard's rule within the limits of experimental errors ($\pm n \times 10^{-3}$ Å) (*40, 41*). The calculations by means of the geometric model (Eq. (22)) show that the maximum positive deviation of the parameters a and c from linearity for intermediate compositions does not exceed 0.012–0.015 Å.

Numerous measurements of the composition dependence of the parameters of the cubic unit cell ($B3$) of ZnS–HgS solid solutions demonstrate agreement with Vegard's rule in the limits of no more than ±0.02 Å (*41*). The calculations by means of Eq. (22) predict the maximum positive deviation for intermediate compositions to be equal to 0.016 Å.

However, in a series of ZnS–γ–MnS solid solutions (structure $B4$) there was observed

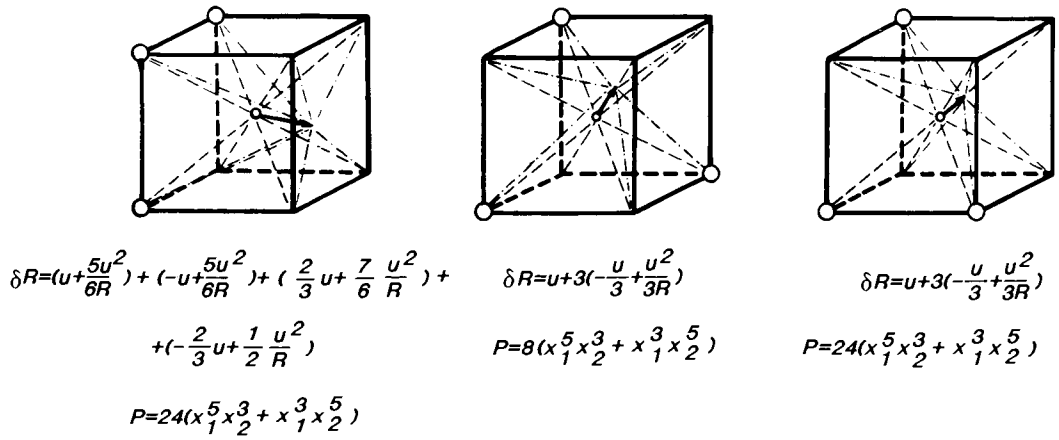

FIG. 10. Cubic arrangements with three substituted ligands and corresponding δR and P.

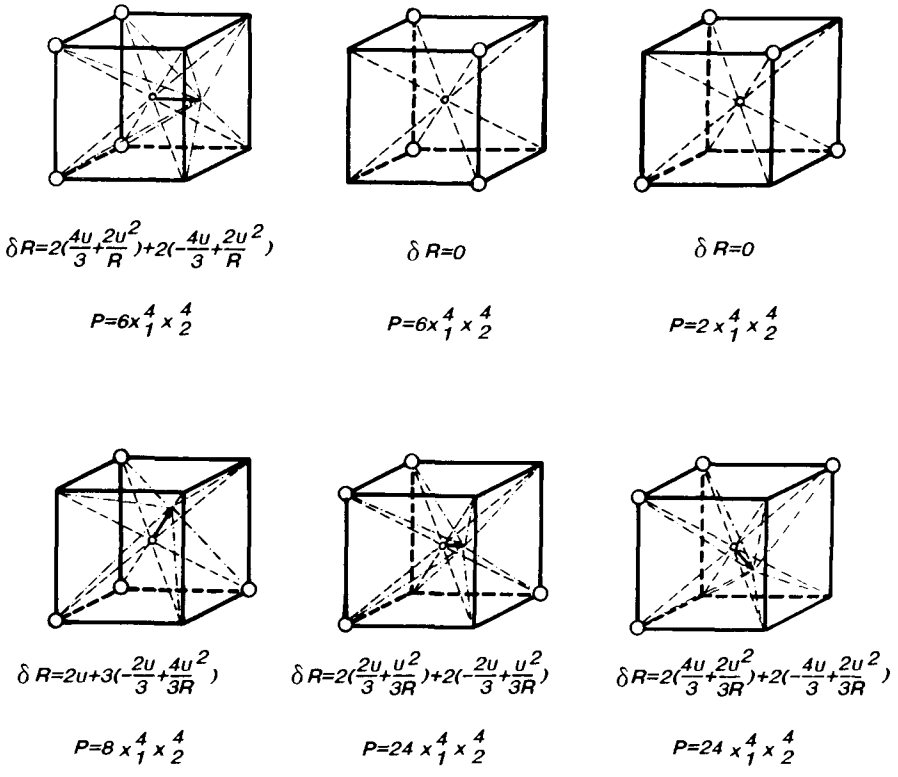

FIG. 11. Cubic arrangements with four substituted ligands and corresponding δR and P.

(*41*) a noticeable positive deviation from the additivity rule of the parameter a; it reached 0.03 Å for intermediate compositions. The geometric model predicts far smaller positive deviations. This observation shows that chemical reasons for deviations of mean interatomic distances from the additivity rule would be additionally analyzed.

It is possible that the accuracy of predictions by the geometric model worsens with

TABLE I

MEASURED AND CALCULATED DEVIATIONS (Å) FROM VERGARD'S RULE

	NaCl–KCl		NaCl–NaBr		KCl–KBr		RbI–RbBr	
x_1	Experimental[a]	Calculated	Experimental[b]	Calculated	Experimental[c]	Calculated	Experimental[d]	Calculated
0.1	0.0045	0.0046	0.0020	0.0013	0.0010	0.0010	—	0.0020
0.3	0.0111	0.0110	0.0035	0.0031	0.0016	0.0023	0.0050	0.0050
0.5	0.0127	0.0133	0.0040	0.0037	0.0023	0.0027	0.0080	0.0060
0.7	0.0105	0.0115	0.0027	0.0031	—	0.0023	0.0040	0.0050
0.9	0.0053	0.0050	0.0012	0.0013	0.0008	0.0010	—	0.0020

[a] Ref. (*34*).
[b] Ref. (*35*).
[c] Ref. (*36*).
[d] Ref. (*37*).

a decrease in the packing density. This model is based on the assumption that a mixed sublattice forms a regular packing; i.e., the coordination polyhedrons around the central atom (in a nonmixed sublattice) are undistorted. In fact, it is not the case as can be seen from the EXAFS data for the InAs–GaAs system (*19*). Thus, the In–In distances are systematically 0.08 Å larger than the Ga–Ga distances for the same compositions of the solid solution, whereas the Ga–In and In–Ga distances are of intermediate values close to the additive values (Fig. 2c). Therefore, solid solution relaxation occurs in both sublattices, though in different degrees, and both primary and secondary changes in bond lengths with respect to those in the end members could be less than those in the geometric model.

It should be noted that deviations from the additivity rule, i.e., from ideality, of geometric characteristics of solid solutions are closely related to nonideality of other properties. In particular, the mixing enthalpy of solid solutions is a function of the square of the size parameter $\Delta R/R$,

$$\Delta H_{\text{mix}} = x_1 x_2 c\,(\Delta R/R)^2, \qquad (29)$$

where c is a semiempirical parameter constant for some groups of crystals (*42*), wherefrom a linear correlation between these quantities follows

$$\delta R/\Delta H_{\text{mix}} = R/K, \qquad (30)$$

where K is an energy parameter. The author hopes to prove in more detail the existence of similar simple correlations between different mixing properties of substitutional solid solutions in another work (*43*).

Acknowledgment

The author expresses his gratitude to I. P. Deineko for help at all the stages of carrying out this work.

References

1. L. Vegard, *Z. Phys.* **5,** 17 (1921).
2. B. J. Pines, *J. Phys. (USSR)* **3,** 309 (1940).
3. J. Friedel, *Philos. Mag.* **46,** 514 (1955).
4. K. A. Gschneider and G. H. Vineyard, *J. Appl. Phys.* **33**(12), 3444 (1962).
5. P. G. Fournet, *J. Phys. Radium* **14,** 374 (1953).
6. W. B. Pearson, "The Crystal Chemistry and Physics of Metals and Alloys," Part 1, Wiley–Interscience, New York (1972).
7. M. Park, T. E. Mitchel, and A. H. Heuer, *J. Am. Ceram. Soc.* **58**(1–2), 43 (1975).
8. H. E. Steinwehr, *Z. Kristallogr.* **125,** 360 (1967).
9. R. C. Newton, and B. J. Wood, *Am. Mineral.* **65,** 733 (1980).
10. N. V. Dergunova, V. P. Sakhnenko, and E. G. Fesenko, *Sov. Phys. Crystallogr.* **23**(1), 94 (1978).
11. V. P. Sakhnenko, E. G. Fesenko, and N. V. Dergunova, *Z. Kristallogr.* **185**(1–4), 530 (1988).
12. V. M. Talanov, *Izv. Akad. Nauk Inorg. Mater.* **16**(8), 1426 (1980).
13. V. M. Talanov, *Phys. Status Solidi B* **106**(1), 99 (1981).
14. V. M. Talanov, *J. Solid State Chem.* **48,** 86 (1983).
15. Z. E-an, *Am. Mineral.* **41,** 523 (1956).
16. J. A. Wasastjerna, *Soc. Sci. Fenn. Commentat Phys. Math.* **13**(5), (1946).
17. K. Huang, *Proc. R. Soc. London A* **190,** 102 (1947).
18. V. I. Iveronova, *Tr. Inst. Kristallogr. Akad. Nauk SSSR* **10,** 339 (1954).
19. J. C. Mikkelsen and J. B. Boyce, *Phys. Rev. B* **28**(12), 7130 (1983).
20. J. B. Boyce and J. C. Mikkelsen, *Phys. Rev. B* **31**(10), 6903 (1985).
21. S. P. Vernon and M. B. Stearns, *Phys. Rev. B* **29,** 6968 (1984).
22. G. S. Durham and J. A. Hawkins, *J. Chem. Phys.* **19,** 2 (1951).
23. J. Hietala, *Ann. Acad. Sci. Fenn., A* **6**(21) (1963).
24. B. G. Dick, T. P. Das, *Phys. Rev.* **127**(4), 1053 (1962).
25. T. B. Douglas, *J. Chem. Phys.* **45**(12), 4571 (1966).
26. J. R. Hardy, *J. Phys. Chem. Solids* **23,** 116 (1962).
27. J. D. Eshelby, *Solid State Phys.* **3,** 79 (1956).
28. W. A. Dollase, *Phys. Chem. Miner.* **6,** 295 (1980).
29. C. K. Shih *et al. Phys. Rev. B* **31**(2), 1139 (1985).
30. V. Hovi, *Ann. Univ. Turkuensis A* **1,** 26 (1957).
31. H. L. Link and L. J. Wood, *J. Am. Chem. Soc.* **62,** 766 (1940).
32. E. B. Thomas and L. J. Wood, *J. Am. Chem. Soc.* **57,** 822 (1935).
33. S. J. E. Callahan and N. O. Smith, *Adv. X-Ray Anal.* **9,** 156 (1966).

34. W. T. Barrett and W. E. Wallace, *J. Am. Chem. Soc.* **76,** 2 (1954).
35. I. E. Nickels, M. A. Fineman, and W. E. Wallace, *J. Phys. Colloid Chem.* **53**(1), 625 (1949).
36. O. D. Slagle and H. A. McKinstry, *Acta Crystallogr.* **21,** 1013 (1966).
37. M. Ahtee, *Ann. Acad. Sci. Fenn. A* **6**(313), 11 (1969).
38. A. Hovi, *Suom. Kemistil. B* **23**(11–12), 80 (1950).
39. T. Teatum and N. O. Smith, *J. Phys. Chem.* **61,** 697 (1957).
40. A. V. Chichagov and L. V. Sipavina, "Lattice Constants of Solid Solutions," Nauka, Moscow (1982) (in Russian).
41. V. L. Tauson and L. V. Chernyshev, "Experimental Studies on Crystal Chemistry and Geochemistry of Zinc Sulfide," Nauka, Novosibirsk (1981) (in Russian).
42. V. S. Urusov, "Theory of Isomorphous Miscibility," Nauka, Moscow (1977) (in Russian).
43. V. S. Urusov, *in* "Advances in Physical Geochemistry" (S. K. Saxena, Ed.), Vol. 10, Springer-Verlag, New York (1991).